Evaluation of corrosion behavior on Mn-Cr austenitic steels using 0.1 M HCl solution

A. Fattah-alhosseini[a,*], B. Izadi[a], M. Asadi Asadabad[b]

[a] *Faculty of Engineering, Bu-Ali Sina University, Hamedan, Iran.*
[b] *Materials Research School, Nuclear Science and Technology Research Institute, Isfahan, Iran.*

ARTICLE INFO

Article history:

Received 3 Jan. 2014
Accepted 1 Feb. 2014
Available online 25 Feb. 2014

Keywords:

Cr-Mn steel
EIS
Acid corrosion

ABSTRACT

One of the attractive low activation steels is the austenitic Mn-Cr steel from the view point of waste disposal because of few long-lived nuclides. In this paper, three types of Mn-Cr austenitic steels were fabricated by vacuum induction furnace. Then plates with 10 mm thickness were produced by hot-rolling. The physical metallurgy of these steels was studied by the corrected Schaeffler diagram, X-ray and electron diffraction patterns. The corrected Schaeffler diagram and X-ray diffraction (XRD) results showed that the matrix of these steels is a single γ-phase structure. Also, the corrosion behaviour in 0.1M HCl solution was evaluated by open-circuit potential, Tafel polarization, and electrochemical impedance spectroscopy (EIS). The results of Tafel polarization experiments showed that corrosion current density of all three Cr-Mn steels is in the range of 10^{-4} A cm^{-2}, which indicates their appropriate resistance in this acidic environment. The Nyquist plots showed that polarization resistance decreases from the first to the third Cr-Mn steels. This trend is due to the increase in corrosion current density which corresponds to Tafel polarization curves.

1. Introduction

Stainless steels are extensively used in industry mainly because of their high resistance to corrosion in many environments. However, due to their high cost, stainless steels cannot be used in applications where they would otherwise be an ideal choice. For this reason, attempts are being made all over the world to produce cheaper stainless steels, at the same time maintaining high corrosion resistance. However, due to their excellent corrosion resistance coupled with ease of weldability and workability, more costly stainless steels are used. The high cost of austenitic stainless steels stems from their relatively high nickel content (8% or more) [1].

In the past 30 years, Fe-Cr-Mn-C alloys have been regarded as possible alternatives to Fe-Cr-Ni-based austenitic stainless steels on the basis of substitution of the strategic element Ni by the more plentiful and cheaper Mn [2-6]. Other advantages of the high-Mn austenitic steels can be found in their applications in wear-resistant and pitting-resistant steel products. High-Mn

Corresponding author:
E-mail address: a.fattah@basu.ac.ir (Arash Fattah-alhosseini).

Table 1. Chemical compositions of three austenitic Mn-Cr steels.

Elements	*C*	*Mn*	*Cr*	*Si*	*P*	*S*	*V*	*Ti*	*Fe*
Mn-Cr Steel-1	0.233	18.54	12.66	0.0676	0.0065	0.0087	0.0721	0.0003	Bal.
Mn-Cr Steel-2	0.053	23.85	11.31	0.776	0.0058	0.0097	0.0479	0.0004	Bal.
Mn-Cr Steel-3	0.294	18.26	10.32	0.103	0.0055	0.0077	0.0501	0.0020	Bal.

steels have also been successfully applied in superconductor industries. This is mainly because of their higher strength in cryogenic environments [7-9].

Various types of low activation austenitic stainless steels have been developed based on Mn–Cr non-magnetic steels [10-12]. Harries et al. and Kohyama et al. [13, 14] have reported that the phase and properties of Mn–Cr steels are unstable under irradiation at high temperature. Although the applicability of the steels to fusion reactor components may be limited due to such characteristics, further investigation is being conducted to optimize their properties and minimize the effects of radiation damage. Shamardin et al. [15] have investigated various types of low activation austenitic stainless steel based on Mn–Cr non-magnetic steels. However, those alloys still have small amounts of Ni, Co, Mo, etc. which cause problems of long-life activation.

In the present study, research has been conducted firstly to eliminate such undesirable elements and produce lower activation austenitic steels that can be manufactured along usual industrial production lines. Also, low-activation austenitic steels frequently come in contact with acids during the processes like cleaning and pickling. In this study, corrosion behavior of low-activation austenitic stainless steel in 0.1M HCl is investigated.

2. Experimental

The three austenitic steels listed in Table 1 were cast and fabricated in the form of a single ingot by vacuum high-frequency induction furnace. The cast ingots were then hot rolled into 40 mm thick slabs and heated to 1200°C for 120 minutes. The acquired plate thicknesses were then further reduced to 30 and finally to 22 mm. Further reduction to 18 and final thickness of 10 mm was achieved after heating the plates at 1100°C for 10 minutes. In order to homogenize the structure, annealing was carried out at 1050°C for 10 minutes and the plates were quenched in water. To examine the structure, XRD evaluations were carried out by a Philips PW-1800, Cu K_{α}.

For electrochemical measurements, test samples were cut from the plates and polished mechanically with wet emery paper up to 2000 grit size on all sides. The polished samples were then embedded in cold curing epoxy resin. Prior to all measurements, working electrodes were degreased with acetone, rinsed with distilled water and dried with a stream of air.

All electrochemical measurements were performed in a conventional three-electrode cell under aerated conditions. The counter electrode was a Pt plate, and all potentials were measured against Ag/AgCl in saturated KCl. The equipment used was μautolab potentiostat/galvanostat controlled by a computer. Prior to all electrochemical measurements, working electrodes immersed at open circuit potential (OCP) for 0.5 h to form a steady-state passive film.

The Tafel curves were recorded by polarizing the specimen to -250 mV cathodically and +250 mV anodically with respect to the OCP at a scan rate of 1 mV s^{-1}. In EIS technique a small amplitude AC signal of 10 mV and frequency spectrum from 100 kHz to 10 mHz were impressed at the OCP and the impedance data were analyzed using Nyquist plots.

3. Results and Discussion

3. 1. Development of Mn-Cr austenitic steels

Mn is an important element in stabilizing the austenite structure. However, an excess amount of Mn accelerates the production of intermetallic compounds and lowers ductility and corrosion resistance [16-18]. Therefore, Mn additions were limited between 15 wt% to

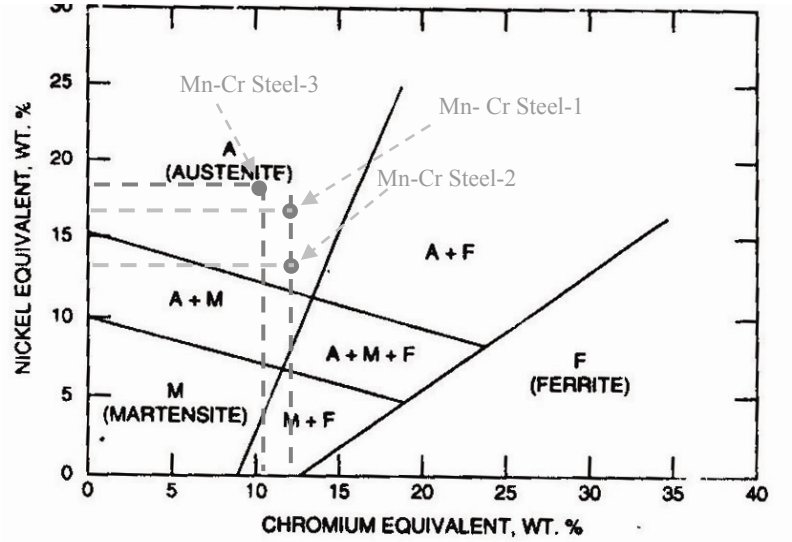

Fig. 1. The corrected Schaeffler diagram for steels containing high amounts of Cr and Mn (maximum 40 wt.% Mn) [18]

35 wt%. On the other hand, a Cr content of more than 11% improves corrosion resistance. An excess amount of Cr destabilizes the austenite structure; therefore, Cr content was limited in the range of 11% to 20%. Si is an effective deoxidizing element. An excess amount of Si, however, leads to destabilization of the austenite structure. As such, the Si content was limited to 1.0%. Reduction of strength caused by the decreased amounts of C and N can be compensated for by adding V, which is intended to precipitate carbide and/or nitride. However, since an excess of V reduces weldability, V was restricted to 0.3%. Adjustment of alloying elements was conducted to obtain a single austenitic phase according to the constitution of austenitic stainless steels, which was based on the constitution diagrams of Schaeffler. Development of the Mn-Cr based stainless steels was done by considering the above factors [19].

The Schaeffler diagram is one of the means of determining the stability of austenite and other phases such as ferrite and martensite in the matrix of stainless steels. For the Schaeffler diagram, the nickel and chromium equivalents were calculated according to the following relationships [20, 21]:

$$Nie = (Ni) + (Co) + 0.5\,(Mn) + 0.3\,(Cu) + 25\,(N) + 30\,(C) \quad [1]$$

$$Cre = (Cr) + 2\,(Si) + 1.5\,(Mo) + 5\,(V) + 5.5\,(A1) + 1.75\,(Nb) + 1.5\,(Ti) + 0.75\,(W) \quad [2]$$

where the concentrations of the respective elements given in parentheses are in weight percent. Klueh et al. [20] illustrated that Schaeffler diagram cannotpredict the amount of phases in steels containing high amounts of Mn and needs some corrections. This led to a new Schaeffler diagram for steels containing high amounts of Cr and Mn (maximum 40 wt.% Mn) as shown in Fig 1.

Table 2 shows the calculated Chromium and Nickel equivalents using relations 1 and 2 for three types of austenitic Mn-Cr steel. It is apparent that in case of using corrected Schaeffler diagram, the matrix of all three steels is single phase austenite. Fig 2 shows the X-ray diffraction patterns of three types of austenitic Mn-Cr steel which presents the XRD patterns of single austenite peak.

3. 2. OCP and Tafel polarization measurements

In Fig 3, changes on OCP of three austenitic steels in 0.1M HCl solution are shown. At the start of immersion, the potential immediately reduces which shows the dissolution of the oxide layer for three austenitic steels. However, as time passes, the open circuit potential is directed towards positive amount. This trend is also reported for austenitic stainless steels in acidic solutions which is indicative of the formation of passive film and its role in increasing protectivity with time [22]. Fig 3

Table 2. The calculated Cr and Ni equivalents for three types of austenitic Mn-Cr steel.

	Mn-Cr Steel-1	Mn-Cr Steel-2	Mn-Cr Steel-3
Cr Equivalent / wt%	12.81	12.86	10.53
Ni Equivalent/ wt%	16.26	13.52	17.95

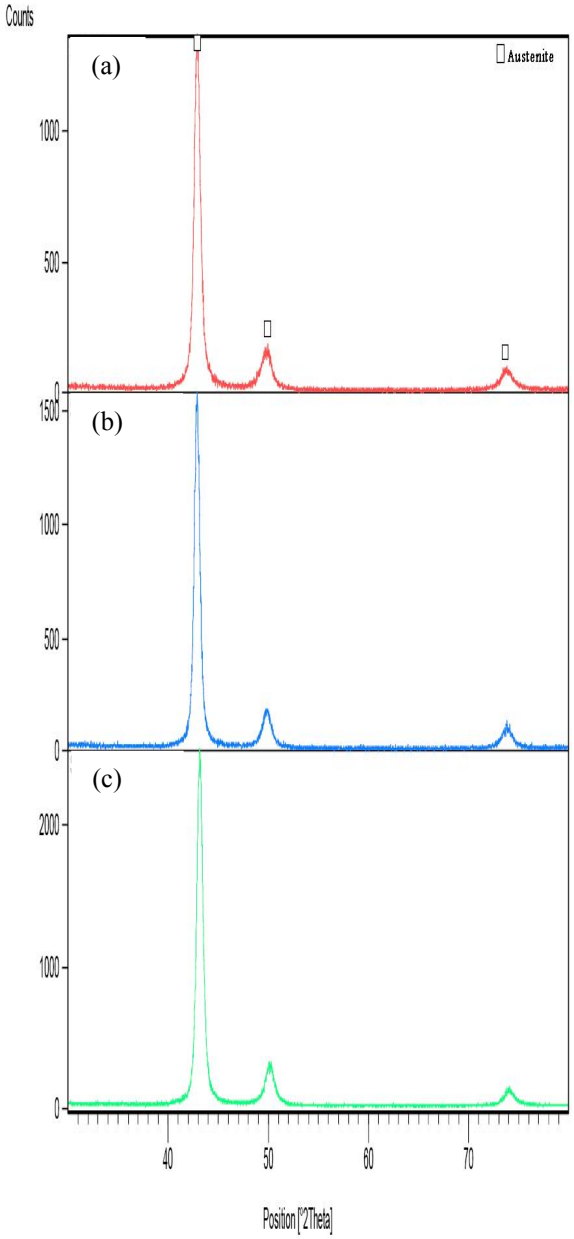

Fig. 2. X-ray diffraction patterns of the fabricated steels: (a) Mn-Cr steel-1, (b) Mn-Cr steel-2 and (c) Mn-Cr steel-3

also indicates that after 30 minutes a complete stable condition is achieved and electrochemical tests are possible.

3. 3. EIS measurements

Nyquist plots of three austenitic Mn-Cr steels in 0.1M HCl solution measured at OCP are given

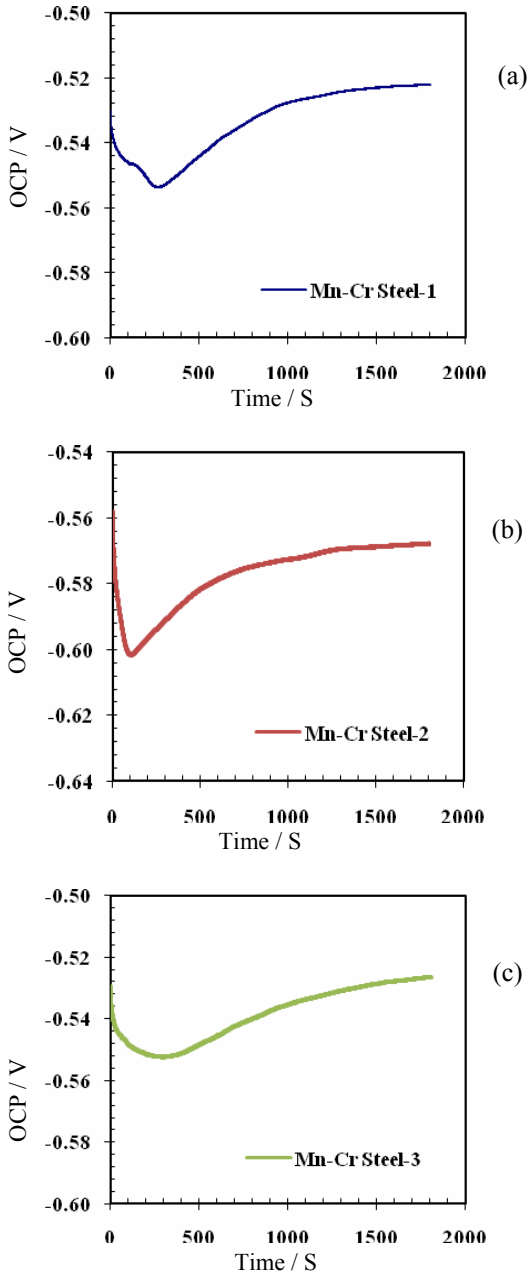

Fig. 3. Open circuit potential (OCP) plots of the fabricated (a) Mn-Cr steel-1, (b) Mn-Cr steel-2 and (c) Mn-Cr steel-3 in 0.1M HCl solution

in Fig 5. These plots were composed of high-frequency capacitive arc and low-frequency small inductive arc. The capacitive arc is associated with the metal dissolution reaction with its diameter being related to the charge transfer resistance (R_{ct}) [23–25]. The polarization resistance was extracted from the diameter of the semicircle in the Nyquist plots. It is seen that the polarization resistance decreases from the first to third Cr-Mn steels, which demonstrates that metal dissolution at the metal/solution interface is facilitated. This trend is due to the increase in corrosion current density which corresponds to Tafel polarization curves.

The increase in the corrosion current density of three austenitic Mn-Cr steels, as shown in Fig 4, is due primarily to the enhancement of metal dissolution associated with the decrease in the R_{ct}. Because three austenitic Mn-Cr steels are composed of various alloying elements,

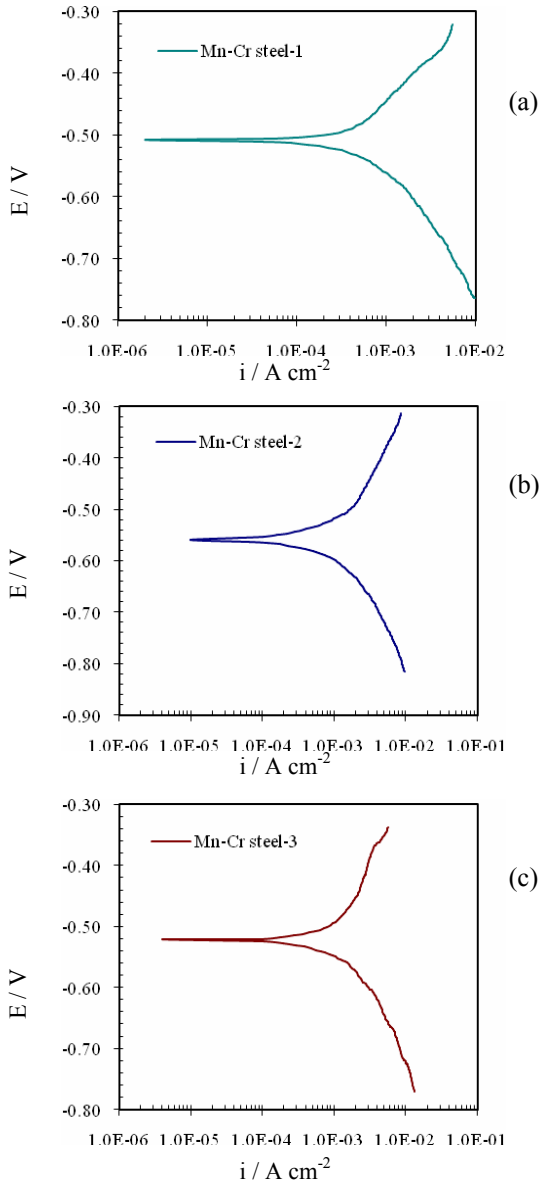

Fig. 4. Tafel plots of the fabricated (a) Mn-Cr steel-1, (b) Mn-Cr steel-2 and (c) Mn-Cr steel-3 in 0.1M HCl solution

not only Fe but also other alloying elements (Cr, Mn) possibly dissolve into the solution. However, R_{ct} is probably governed by Fe dissolution, because Fe is the major alloying element [25].

The inductive small arc in the impedance spectra of three austenitic Mn-Cr steels suggests that Mn enhances the activity of the iron adsorbed intermediate (Fe(I)ad) or generates another adsorbed species acting as a dissolution intermediate like Fe(I)ad, which is considered to be manganese adsorbed species, thereby increasing the dissolution rate of Fe [25]. Also, from the effects of Mn on the active dissolution behavior of three austenitic Mn-Cr steels in 0.1M HCl solution, it can be analogically inferred that Mn facilitates metal dissolution inside the pit by enhancing the activity of iron adsorbed intermediate or generating second intermediate species (possibly manganese adsorbed intermediate) acting as another dissolution path [23-25].

4. Conclusions

The corrosion behavior of three austenitic

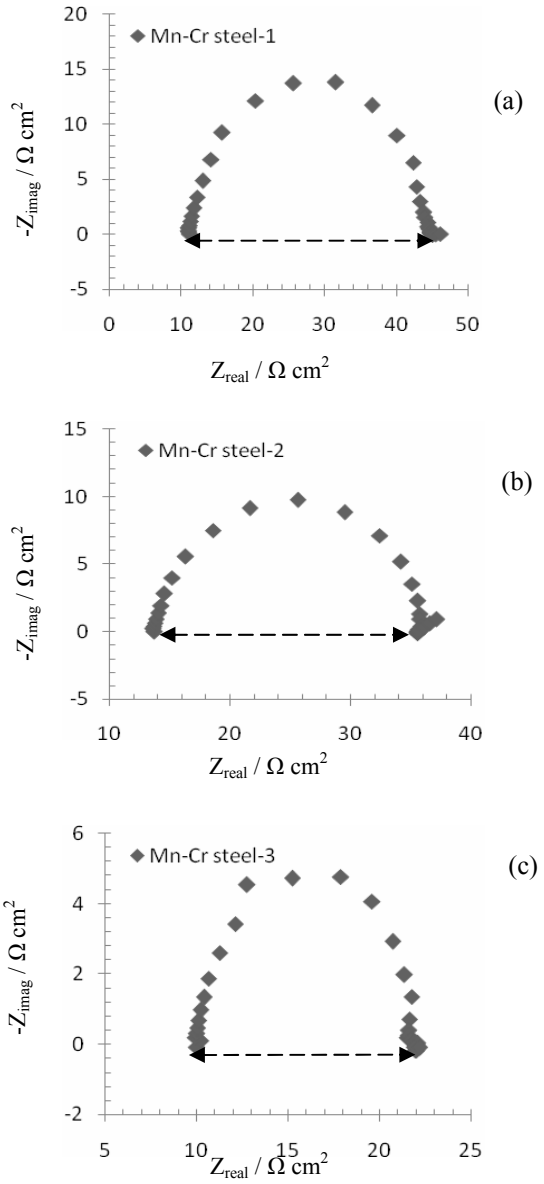

Fig. 5. Nyquist plots of the fabricated (a) Mn-Cr steel-1, (b) Mn-Cr steel-2 and (c) Mn-Cr steel-3 in 0.1M HCl solution

Mn-Cr steels in 0.1M HCl solution was investigated in the present work. Conclusions drawn from the study are as follows:

1. The amounts of nickel and chromium equivalents as well as the corrected Schaeffler diagram show austenite to be the only microstructure of three Mn-Cr steels. This is also confirmed by XRD evaluations.
2. The results of Tafel polarization curves show that corrosion current density of all three Cr-Mn steels is in the range of 10^{-4} A cm^{-2}, which indicates their appropriate resistance in acidic environment.
3. The reason for increased current density from the first to the third of Cr-Mn steels is directly related to the reduction of chromium.
4. The results of impedance plots in 0.1M HCl solution showed that polarization resistance from the first to the third Cr-Mn steels decreases. This trend is due to the increase in corrosion current density which corresponds to Tafel polarization curves.

References

1. M. Kemp, A. van Bennekom, F. P. A. Robinson, "Evaluation of the corrosion and mechanical properties of a range of experimental Cr-Mn stainless steels", Mater. Sci. Eng. A, 199, 1995, pp. 183–194.
2. B. R. Nijhawan, in Stainless Steels `87. The Institute of Metals, York, 1987, p. 535.
3. R. A. Lula, in Manganese Stainless Steels. The Manganese Centre, Paris, 1986, p. 1.
4. S. R. Chen, H. A. Davies, W. M. Rainforth, "Austenite phase formation in rapidly solidified Fe-Cr-Mn-C Steels", Acta mater. 47, 1999, pp. 4555–4569.
5. Y. S. Zhang, X. M. Zhu, S. H. Zhong, "Effect of alloying elements on the electrochemical polarization behavior and passive film of Fe–Mn base alloys in various aqueous solutions", Corros. Sci. 46, 2004, pp. 853–876.
6. H. Y. Bi, X.X. Jiang, S. Z. Li, "The corrosive wear behavior of Cr–Mn–N series casting stainless steel", Wear, 225–229, 1999, pp. 1043–1049.
7. U. R. Lenel, B. R. Knott, "Structure and properties of corrosion and wear resistant Cr-Mn-N steels", Metall. Trans., 18 A, 1987, pp. 847–855.
8. Y. Okazaki, K. Miyahara, N. Wade, Y. Hosoi, "Effect of manganese and chromium on microstructure and toughness of Fe-Cr-Mn alloys resulting from solid-solution treatment", J. Japan. Inst. Metals, 53, 1989, pp. 502–511.
9. H. Masumoto, K. Suemune, H. Nakajima, S. Shimamoto, "Development of a high-strength high-manganese stainless steel for cryogenic use", Adv. Cryogenic Engng Mater., 30, 1984, pp. 169–176.
10. P. Schiller, "Review of materials selection for fusion reactors", J. Nucl. Mater. 206, 1993, pp. 113–120.
11. K. Miyahara, D. S. Bae, T. Kimura, Y. Shimoide, Y. Hosoi, "Strength properties and microstructure of high Mn–Cr austenitic steels as potential high temperature materials", ISIJ Int. 37, 1996, pp. 878–882.
12. B. Hu, H. Kinoshita, T. Shibayama, H. Takahashi, "Effect of helium on radiation behavior in low activation Fe–Cr–Mn alloys", Mater. Trans. 43, 2002, pp. 622–626.
13. D. R. Harries, G. J. Butterworth, A. Hishinuma, F. W. Wiffen, "Evaluation of reduced-activation options for fusion materials development", J. Nucl. Mater. 191–194, 1992, pp. 92–99.
14. A. Kohyama, M. L. Grossbeck, G. Piatti, "The application of austenitic stainless steels in advanced fusion systems: current limitations and future prospects", J. Nucl. Mater. 191–194, 1992, pp. 37–44.
15. V. K. Shamardin, T. M. Bulanova, V. N. Golovanov, V. S. Neustroyev, A. V. Povstyanko, Z. E. Ostrovsky, "Change in the properties of Fe-Cr-Ni and Fe-Cr-Mn austenitic steels under mixed and fast neutron irradiation", J. Nucl. Mater. 233–237, 1996, pp. 162–168.
16. Y. S. Lim, J. S. Kim, S. J. Ahn, H. S. Kwon, Y. Katada, The influences of microstructure and nitrogen alloying on pitting corrosion of type 316L and 20 wt.% Mn-substituted type 316L stainless steels, Corros. Sci. 43, 2001, pp. 53–68.
17. A. S. Hamada, L. P. Karjalainen, R. D. K. Misra, J. Talonen, "Contribution of deformation mechanisms to strength and ductility in two Cr–Mn grade austenitic stainless steels", Mater. Sci. Eng. A, 559, 2013, pp. 336–344.
18. A. I. Z. Farahat, O. Hamed, A. El-Sisi, M. Hawash, "Effect of hot forging and Mn content on austenitic stainless steel containing high carbon", Mater. Sci. Eng. A, 530, 2011, pp. 98–106.
19. M. Onozuka, T. Saida, S. Hirai, M. Kusuhashi, I. Sato, T. Hatakeyama, "Low-activation Mn–Cr austenitic stainless steel with further reduced content of long-lived radioactive elements", J. Nucl. Mater. 255, 1998, pp. 128–138.
20. R. L. Klueh, P. J. Maziasz, E. H. Lee, "Manganese as an Austenite Stabilizer in Fe-Cr-Mn-C Steels", Mater. Sci. Eng. A, 102, 1988, pp. 115–124.
21. M. Foldefiki, H. Ledbetter, P. Uggowitzer, "Magnetic properties of Cr-Mn austenitic stainless steels", J. Magnetism Magnet. Mater. 110, 1992, pp. 185–196.
22. G. Ruhi, O. P. Modi, I. B. Singh, "Pitting of

AISI 304L stainless steel coated with nano structured sol–gel alumina coatings in chloride containing acidic environments", Corros. Sci. 51, 2009, pp. 3057–3063.

23. R. F. A. Jargelius-Pettersson, B. G. Pound, "Examination of the Role of Molybdenum in Passivation of Stainless Steels Using AC Impedance Spectroscopy", J. Electrochem. Soc. 145, 1998, pp. 1462–1469.
24. A. Pardo, M. C. Merino, A. E. Coy, F. Viejo, R. Arrabal, E. Matykina, "Effect of Mo and Mn additions on the corrosion behaviour of AISI 304 and 316 stainless steels in H_2SO_4", Corros. Sci. 50, 2008, pp. 780–794.
25. K. J. Park, H. S. Kwon, "Effects of Mn on the localized corrosion behavior of Fe–18Cr alloysμ, Electrochim. Acta 55, 2010, pp. 3421–3427.